

Enhanced ferromagnetism and spin-polarized tunneling studies in Co-Mn alloy films

Tae Hee Kim and Jagadeesh S. Moodera

Francis Bitter Magnet Lab, Massachusetts Institute of Technology, Cambridge, Massachusetts 02139

(Received 7 August 2002; published 30 September 2002)

Enhanced ferromagnetism is observed for extended alloy compositions in $\text{Co}_{1-x}\text{Mn}_x$ ($x=0.1-0.7$) films grown in ultraclean conditions at liquid nitrogen temperature. For these alloys, high values of spin polarization were also measured using the Meservey-Tedrow technique of spin-polarized tunneling. Ferromagnetic behavior exists even in $\text{Co}_{0.3}\text{Mn}_{0.7}$ alloy films, where earlier bulk studies show only antiferromagnetic behavior for alloy compositions with $x>0.3$. X-ray diffraction and transmission electron microscopy data show a metastable fcc phase for our films, which is likely responsible for the enhanced magnetic moment. Our work shows the importance of the local environment of Mn, which is expected to dictate the magnetic interactions in these alloys.

DOI: 10.1103/PhysRevB.66.104436

PACS number(s): 75.70.-i, 81.05.Zx, 72.25.-b, 75.50.-y

INTRODUCTION

The molecular beam epitaxy (MBE) film growth technique offers ample opportunities for exploring the relation between novel structures and magnetism. In the past decade nonequilibrium phases of transition metals [bcc Ni (Ref. 1) or Co (Ref. 2), hcp Fe (Ref. 3) bcc or fcc Mn (Refs. 4 and 5), for example] have been stabilized in thin-film form by MBE growth. Because of the exotic structural and magnetic properties, Mn is an interesting candidate for thin-film growth, as it is expected to show different local spin configurations. Until now, there has been only limited information on the structure of Mn films on metallic substrates. Previous studies of Mn overlayers on Ru(001) (Ref. 4), Ag(001) (Ref. 5), Pd(111) (Ref. 6), and Fe(001) (Ref. 7) substrates have made efforts to expand the Mn lattice to produce large magnetic moments approaching the Hund's rule limit of $5\mu_B$. For such metastable structures of $3d$ elements and compounds, theoretical predictions of the ground-state properties have shown various magnetic properties including a dramatic variation in magnetic moments (M_s), unusual magnetic anisotropy in ultrathin films, and even ferro- or antiferromagnetic ordering for expanded lattice materials that are normally nonmagnetic.^{8,9} Based on the local density approximation (LDA), total energy calculations as a function of the lattice constant have predicted magnetically ordered bcc and fcc phases of Mn above some minimum lattice constants: the bcc Mn phase is expected to have a ferromagnetic ground state for $a_0 \geq 2.75 \text{ \AA}$, while in the fcc Mn phase an antiferromagnetic ground state occurs for $a_0 \geq 3.85 \text{ \AA}$.⁸

Mn impurities in various host materials such as Co, Ni-Co, or Ni-Fe have also been investigated theoretically, concentrating on the local spin structure of Mn with respect to the host atoms.^{8,10,11} Direct experimental observation of the ground-state properties of those materials may be difficult since their magnetic or crystallographic structures are not very stable under ambient conditions. In the past, materials such as fcc or bcc Co (or Mn) and fcc or bcc CoMn (or CoFe) alloys have been studied experimentally to investigate the role of the host atoms on the spin structure of Mn atoms.^{12,13}

Our aim was to study the magnetic properties in nonequi-

librium phases of transition metals, with a view to modulate the d -like conduction-electron (or sp -electron) spin polarization in a controlled manner in this case using Mn (antiferromagnetic and with large d -like conduction electrons) and Co (ferromagnetic and with fewer itinerant d electrons) (Ref. 14) in $\text{Co}_{1-x}\text{Mn}_x$ alloy films. We investigated their structural and magnetic properties for selected Mn concentrations, including the degree of spin polarization of tunneling electrons by the Meservey-Tedrow technique using $\text{Al}/\text{AlO}_x/\text{Co}_{1-x}\text{Mn}_x$ junctions.¹⁵

EXPERIMENTS

Thin films of $\text{Co}_{1-x}\text{Mn}_x$ ($x=0.1-0.7$) were grown by coevaporation of Co and Mn under UHV conditions. The base pressure inside the chamber was below 2×10^{-10} Torr and less than 5×10^{-9} Torr during film deposition. Co-Mn films about 200 \AA thick were grown on glass or unetched Si wafer cooled to liquid nitrogen temperature. The film composition and uniformity were controlled to better than $\pm 1.0\%$ by two independent quartz crystal rate monitors and also by keeping the deposition rate low, $\sim 0.03-0.5 \text{ \AA/s}$. We confirmed that the nominal composition of films, by using surface-sensitive Auger electron spectroscopy as well as Rutherford backscattering, was the same as the desired composition within about 2% error.

$\text{Co}_{1-x}\text{Mn}_x$ films of 200 \AA thickness were deposited on (100) or (111) Si for magnetization measurements, covered with a protective layer of 50 \AA Al_2O_3 . Trilayer junctions for spin-polarized tunneling measurements were fabricated by using metal shadow masks as follows: A narrow strip of Al film, 40 \AA thick, was deposited onto the liquid-nitrogen-cooled glass substrate. After warming it to room temperature, the Al surface was oxidized in oxygen plasma in the load lock chamber to create the insulating tunnel barrier. This was followed by depositing the $\text{Co}_{1-x}\text{Mn}_x$ (200 \AA) counterelectrode cross strips in the main chamber to complete the junction $\text{Al}/\text{Al}_2\text{O}_3/\text{Co}_{1-x}\text{Mn}_x$. Al_2O_3 of 80 \AA was deposited on the oxidized bottom electrode to define a small window in the junction area to avoid edge effects before $\text{Co}_{1-x}\text{Mn}_x$ was deposited.

Structural analysis of the deposited films was carried out

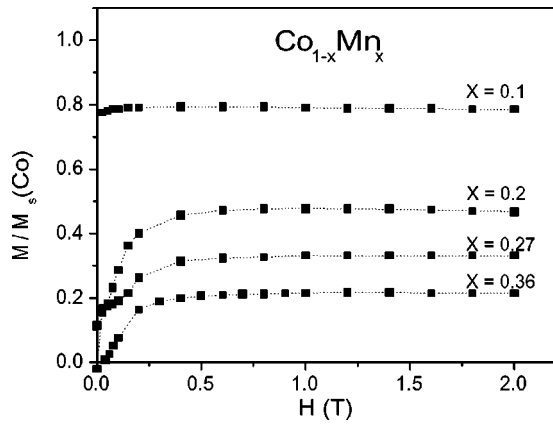


FIG. 1. Magnetization as a function of the applied field at 5 K for the $\text{Co}_{1-x}\text{Mn}_x$ films ($x = 0.1, 0.2, 0.27,$ and 0.36), normalized by the saturation magnetization value of Co.

using the x-ray powder diffraction technique with Cu $K\alpha$ radiation and a graphite monochromator. For transmission electron microscopy studies, films were prepared on C- or SiO-coated transmission electron microscope (TEM) grids. Films were deposited onto liquid-nitrogen-cooled grids just as in the case of the films prepared for the magnetic studies. A Jeol 2010 TEM operating at 200 kV was used to observe the grain structure, compositional homogeneity, and crystal structure of these films.

Magnetization data were taken using a Quantum Design superconducting quantum interference device (SQUID) magnetometer. After cooling the sample to 5 K in zero field, the magnetic hysteresis loops were traced with an applied field up to 2 T. The degree of spin polarization in the alloy films was determined using the Meservey-Tedrow technique. Here the tunnel junctions were cooled to about 0.4 K and tunneling conductance data were taken as a function of dc bias in the mV range without or with an applied field of a few tesla parallel to the film plane.

RESULTS AND DISCUSSION

Magnetic hysteresis loops for various Co-Mn alloys were measured at 5 and 295 K. Shown in Fig. 1 is the M vs H data at 5 K for Co-Mn alloys, with Mn concentrations ranging from 10% to 36%, normalized by the saturation value of Co (1422 emu/cm^3). It can be seen that the alloys with 10–36 at. % Mn are ferromagnetic at 5 K with a fairly high remanent magnetization, although the magnetization values are smaller than for that of Co.

The ferromagnetic behavior persists at 295 K even for higher Mn concentrations of up to 70 at. % of Mn, as shown in Fig. 2. For $\text{Co}_{0.5}\text{Mn}_{0.5}$, the hysteresis loop at 295 K shows the characteristics of a soft ferromagnet, while the saturation was not reached in field up to 2 T at 5 K. This probably shows that a frustrated spin state exists in this alloy, which can occur as a result of having a mixed exchange interaction ($J < 0$ and > 0) between the atoms. Such a coexistence of both signs of the exchange interaction has been reported in the binary alloys such as Ni-Mn where for some concentrations a ferromagnetic to antiferromagnetic phase transition

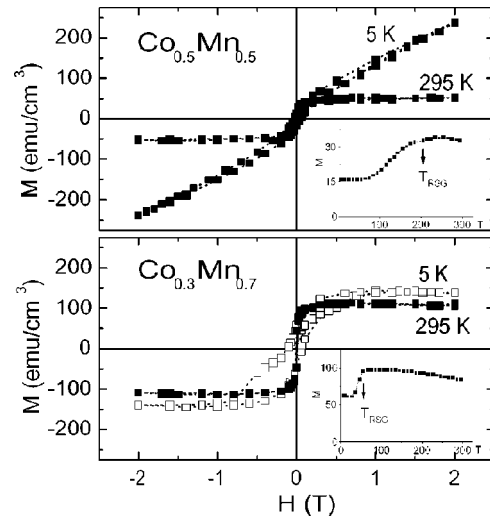


FIG. 2. Hysteresis loop of Co-Mn alloy measured at 5 K (open square) and 295 K (solid square) for (a) 50 at. % Mn and (b) 70 at. % Mn. In the inset, ZFC temperature-dependent magnetization curves (in units of emu/cm^3) are shown for these two alloy compositions.

appears without the structural transformations.^{16,17} In the insets of Figs. 2(a) and 2(b), the zero-field-cooled (ZFC) temperature-dependent magnetization measured at 0.05 T shows a sharp decrease below 50 K for $\text{Co}_{0.3}\text{Mn}_{0.7}$ and a gradual decrease below 200 K for $\text{Co}_{0.5}\text{Mn}_{0.5}$. This is reminiscent of the existence of the mixed magnetic phase, the so-called reentrant spin-glass (RSG) phase.¹⁸ We take the transition temperature (T_{RSG}) to be the point where ZFC $M(T)$ shows the sharpest drop. The RSG phase was also observed for 30 at. % Mn alloy below 100 K in low applied field (0.05 T). In the whole range of Mn concentration from 10% to 70%, the films were ferromagnetic above 300 K. The magnetization curves displayed the typical ferromagnetic behavior at 300 K, whereas the bulk magnetic phase diagram shows antiferromagnetic behavior for Mn concentrations $> 30\%$. Thus it is clear that the ferromagnetic phase is extended in our films and is in stark contrast with the bulk phase diagram.¹⁹ In the bulk, at 32% of Mn concentration the ferromagnetic long-range order disappears, and above, 42% the antiferromagnetic long-range order appears.^{12,19}

In Fig. 3 we compare the magnetic moments obtained (saturation value and for $x = 0.5$ and 0.7 M value at 2 T) as a function of Mn concentration for our Co-Mn alloy films with those reported by other groups for bulk¹⁹ as well as thin films.²⁰ One can clearly see that the magnetic moment has been enhanced in our films in the range from 27% to 70% concentration of Mn. In fact, for our films with Mn concentration above 25%, the magnetic moments are considerably higher than those in bulk. Rogers *et al.* also reported a three-fold enhancement in saturation magnetization for the $\text{Co}_{0.75}\text{Mn}_{0.25}$ thin films deposited by rf magnetron sputter deposition at 300 °C (also shown in Fig. 3), while such a large enhancement was not observed for films grown at room temperature.²⁰ In their work, the large M_s value for the films deposited at elevated substrate temperature was attributed to the occurrence of drastic compositional segregation into dis-

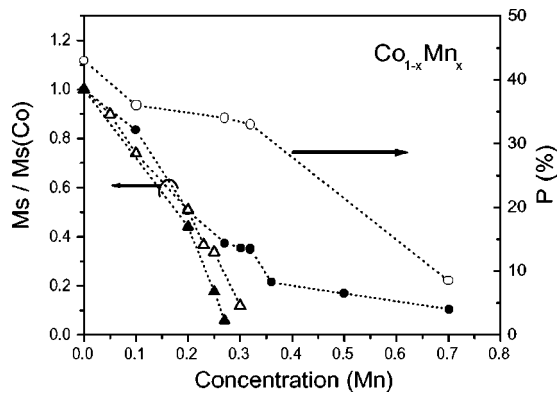


FIG. 3. Dependence of saturation magnetization and spin polarization on Mn content: saturation magnetization data for the present work (solid circle); films deposited by sputtering at room temperature from Ref. 20 (open triangle); bulk Co-Mn alloy samples from Ref. 19 (solid triangle). Spin polarization values obtained in the present work are also shown (open circle). Lines are a guide to the eye.

tinct Co-rich and Mn-rich components. The large magnetic moment has also been reported for overlayers and sandwiched layers of bcc Co and fcc or bct Mn,⁴ as well as for Co/Mn multilayers.²¹ The behavior in the latter system has been attributed to Mn layers adjacent to Co layers contributing ferromagnetically to the magnetic moment. Our films are quench condensed onto the liquid-nitrogen-cooled surface, which should result in structural and compositional homogeneity as well as drastically reduced possibilities for phase segregation. The homogeneity and compositional uniformity of our film surface was evidenced by *in situ* Auger spectroscopy as well as TEM studies. Within the limits of these techniques, the alloys had the same concentration of the components as indicated by the quartz crystal monitors. Additionally, we also observed very similar magnetic behavior for films prepared at room temperature.

The tunnel conductance as a function of voltage for the Al/Al₂O₃/Co_{1-x}Mn_x junction was measured at 0.4 K. In zero field the conductance curve showed typical behavior for the case when Al is superconducting with negligible conductance at zero bias, with a rapid increase when the voltage reached the superconducting energy gap of Al. In high applied fields (3.3 and 3.6 T) the conductance curves showed Zeeman splitting of the quasiparticle density of states of superconducting Al, as well as the asymmetry in conductance due to the spin polarization (P) of tunneling electrons.¹⁵ The experimental conductance data for various applied fields were fitted to Maki's theory (taking into account spin-orbit scattering correction) to extract P values uniquely.

For the Co-Mn system, the spin polarization of the tunneling electrons, as determined above, for the various Mn concentrations is also shown in the Fig. 3. Polarization values of 37% and 33% were observed for 10% and 27% of Mn concentrations, respectively. It is remarkable to see a polarization of 9% for the alloy with even at 70% Mn concentration, whereas this alloy has negligible magnetic moment ($0.3\mu_B$). This result is consistent with the ferromagnetic behavior observed by the magnetization curve at 5 K.

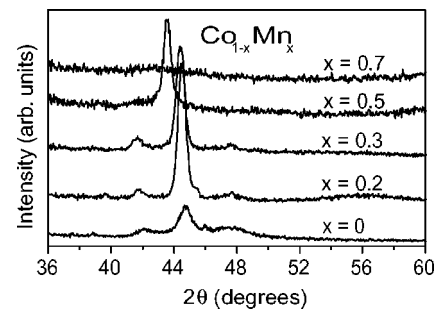


FIG. 4. X-ray powder diffraction data for the Co_{1-x}Mn_x films ($x=0, 0.2, 0.3, 0.5, \text{ and } 0.7$).

Stepanyuk *et al.*¹¹ have pointed out the possible dependence of the nature of the magnetic interaction on the structural variation in Mn-doped Co. Based on this model, one can see that the surface may behave differently from the bulk. The P values shown are the average values obtained from the three independent junctions for each alloy composition. Thus one can see that the polarization decreases very slowly from 43% to 33% with increasing Mn concentrations up to 32%, followed by a larger decrease for the higher Mn concentration, as the magnetic moment varies. It is well known that the spin polarization values obtained here reflect the behavior of the tunneling electrons coming from the magnetic layers adjacent to the barrier and thus strongly reflect the surface/interface magnetic property of the Co-Mn alloy system.^{15,22} As the *in situ* Auger spectroscopic analysis showed the surface alloy composition to be similar to the bulk, surface segregation is ruled out within the limit of this experimental technique.

In order to understand the origin of the large enhancement of the magnetic moment for Mn concentrations above 25%, the structure of our films was investigated by x-ray powder diffraction for different Mn concentrations. As shown in Fig. 4, except for Co_{0.3}Mn_{0.7}, all samples showed one diffraction peak appearing between 43.5° and 44.8° for various alloy concentrations. These peaks do not correspond to Mn (bcc or fcc) or Co (hcp or fcc) powder diffraction data. If we assume our films to have fcc structure based on earlier thin-film and bulk studies of Co-Mn alloys,²⁶ the peak in the range from 43.5° to 44.5° could correspond to (111) orientation with a lattice parameter of 3.6–3.5 Å. These lattice parameters are similar to that of bulk fcc structure (3.56–3.61 Å),^{19,21,26} indicating that for $0.1 < x \leq 0.5$ our Co_{1-x}Mn_x alloy films appear to have fcc structure.

TEM studies were carried out to further support the structural identification. This showed that the films were homogeneous in composition with no phase segregation. In the alloys the grains were significantly larger than that for pure Co film. The electron diffraction patterns for Co, Co_{0.9}Mn_{0.1}, and Co_{0.5}Mn_{0.5} films are shown in Fig. 5. The fcc structure was observed for Co as well as alloy films, though strikingly Co was polycrystalline, and the alloy films showed near epitaxial growth. Additionally, in the case of the alloys, the diffraction patterns show a *distorted* fcc (or can also be fct²³) structure, the distortion increasing as the Mn concentration increased.²⁴ This confirms the interpretation of the XRD data.

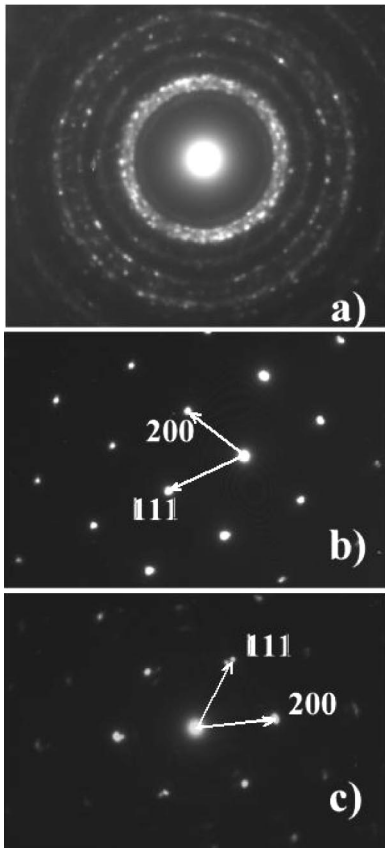


FIG. 5. Plane-view electron diffraction patterns for thin films of (a) pure Co, (b) $\text{Co}_{0.9}\text{Mn}_{0.1}$ alloy, and (c) $\text{Co}_{0.5}\text{Mn}_{0.5}$ alloy deposited at liquid nitrogen temperature onto a silicon-oxide-coated Cu grid.

The magnetic phase diagram in the bulk Co-Mn system investigated by Menshikov *et al.*¹⁶ shows that $\text{Co}_{1-x}\text{Mn}_x$ is ferromagnetic with hcp or fcc structure for $0 < x \leq 0.32$, whereas it is antiferromagnetic with fcc structure for $0.32 < x \leq 0.52$. For $x > 0.52$, it was no longer possible to stabilize the fcc structure. Our structural and magnetic analyses thus show that a new ferromagnetic phase with fcc structure is formed in the wide Mn concentration range $0.1 \leq x < 0.7$ by the quench-condensed growth technique under clean conditions.

In these fcc Co-Mn alloys the rich diversity of magnetic behavior arising from competing exchange interactions has been studied continuously for the last three decades. For fcc Co-Mn bulk alloys, earlier neutron diffraction experiments showed a ferromagnetic exchange interaction between Co and Mn atoms in the concentration range between ferro- and antiferromagnetic long-range-ordered phases.^{25,26} In this concentration region from 25 to 40 at. % Mn, Cable and Tsunoda have reported a small ferromagnetic moment at the Mn sites ($\sim 0.3\mu_B$) for single-crystal samples.²⁶ Our data indicate several possibilities: (i) The Co moment is reduced upon alloying with Mn, (ii) Mn carries a moment and at least some of them if not all are aligned antiparallel with Co, and (iii) itinerant mediation of the exchange interaction between local moments is significantly modified.¹⁴

In a recent work using x-ray magnetic circular dichroism (XMCD), for the eight-monolayer-thick $\text{Co}_{1-x}\text{Mn}_x$ alloy

films ($0.02 \leq x \leq 0.21$) grown on Cu(100) substrates, the existence of the ferromagnetically coupled Co and Mn moments has been reported.²⁷ However, this parallel coupling between Co and Mn moments disappeared for the bulklike thick films (50 monolayers), whereas for ultrathin films, with increasing Mn concentration, the magnitude of average Mn and Co moments decreased, finally reaching zero moment for both Mn and Co when the Mn concentration becomes higher than 18%. These results of neutron and XMCD studies strongly suggest to us that such a positive exchange interaction between Co and Mn can lead to a large enhancement of the magnetic moment in Co-Mn alloy films. Preliminary XMCD data for $\text{Co}_{0.8}\text{Mn}_{0.2}$ film (200 Å thick) shows a ferromagnetic alignment between Co and Mn atoms.²⁸ A detailed investigation using XMCD for various Mn concentrations will be published separately.

The influence of local environment of Mn for the exotic magnetic behavior has been investigated earlier in Co(Ni)-Mn multilayers,¹⁴ as well as in different Mn alloys. As mentioned previously, it is well known that Mn can be in a number of different structural configurations and have a wide range of atomic volumes. Four different structures have been reported in bulk at different temperatures. The α and β phases are complex cubic structures with 58 and 20 atoms per unit cell, respectively, whereas γ and δ phases are fcc and bcc with lattice parameters of 2.73 and 2.67 Å, respectively.²⁹ The perpendicular anisotropy was reported at interfaces in Co(Ni)-Mn multilayers, which was attributed to the large number of *d*-like conduction electrons in Mn, as compared to Fe, Co, and Ni. The perturbation of the itinerant *d* electrons both in Co and Mn can be expected to play a significant role in the enhanced ferromagnetism seen in our Co-Mn alloys.^{8,11,30,31} This may be well served by having a clean and homogeneous material and forming in an fcc phase. It can be an interesting theoretical problem that may lead to further predictions.

In summary, the large enhancement of magnetic moment was found with significant spin polarization values for $\text{Co}_{1-x}\text{Mn}_x$ ($0.1 < x \leq 0.7$) alloy films grown in an UHV environment at liquid nitrogen temperature. For $0.2 < x \leq 0.7$, a ferromagnetic phase with fcc structure has been obtained in thin films of the alloy, whereas the ferromagnetic fcc phase for bulk has been observed only in the narrow intermediate range ($0.25 < x \leq 0.42$) between ferromagnetic and antiferromagnetic long-range-ordered phases. We believe that the local environment as well as the *d*-band structure of Mn dictates the magnetic properties. The possibility for stabilizing a metastable phase, the ferromagnetic fcc phase, with an enhanced magnetic property was shown in this Co-Mn system.

ACKNOWLEDGMENTS

This work has been supported by NSF Grant Nos. DMR 9730908 and 0137632 and ONR Grant No. N00014-J-92-1847.

- ¹B. Heinrich, S. T. Purcell, J. R. Dutcher, K. B. Urquhart, J. F. Cochran, and A. S. Arrott, *Phys. Rev. B* **38**, 12 879 (1988).
- ²G. A. Prinz, *Phys. Rev. Lett.* **54**, 1031 (1985).
- ³M. Maurer, J. C. Ousset, M. F. Ravet, and M. Piecuch, *Europhys. Lett.* **9**, 803 (1989).
- ⁴A. S. Arrott, B. Heinrich, S. T. Purcell, J. F. Cochran, and K. B. Urquhart, *J. Appl. Phys.* **61**, 3721 (1988); B. Heinrich, A. S. Arrott, C. Liu, and S. T. Purcell, *J. Vac. Sci. Technol. A* **5**, 1935 (1988).
- ⁵B. T. Jonker, J. J. Krebs, and G. A. Prinz, *Phys. Rev. B* **39**, 1399 (1989).
- ⁶D. Tian, H. Li, S. C. Wu, F. Jona, and P. M. Marcus, *Phys. Rev. B* **45**, 3749 (1992).
- ⁷G. A. Prinz, *Mater. Res. Bull.* **13**, 28 (1988).
- ⁸V. L. Moruzzi, P. M. Marcus, K. Schwarz, and P. Mohn, *Phys. Rev. B* **34**, 1784 (1986); V. L. Moruzzi and P. M. Marcus, *ibid.* **38**, 1613 (1988).
- ⁹J. L. Fry, Y. Z. Zhao, N. B. Brener, G. Fuster, and J. Callaway, *Phys. Rev. B* **36**, 868 (1987); G. Fuster, N. B. Brener, J. Callaway, J. L. Fry, and Y. Z. Zhao, *ibid.* **38**, 423 (1988).
- ¹⁰J. Kübler, *Physics B* **127**, 257 (1984).
- ¹¹V. S. Stepanyuk, R. Zeller, P. H. Dederichs, and I. Mertig, *Phys. Rev. B* **49**, 5157 (1994).
- ¹²M. Acet, C. John, and E. F. Wassermann, *J. Appl. Phys.* **70**, 6556 (1991).
- ¹³G. A. Prinz, in *Ultrathin Magnetic Structures II*, edited by B. Heinrich and J. A. C. Bland (Springer-Verlag, Berlin, 1994).
- ¹⁴M. B. Stearns, *J. Appl. Phys.* **53**, 2436 (1982); C. B. Zimm and M. B. Stearns, *J. Magn. Magn. Mater.* **50**, 223 (1985).
- ¹⁵R. Meservey and P. M. Tedrow, *Phys. Rep.* **238**, 173 (1994).
- ¹⁶A. Z. Menshikov, V. A. Kazantsev, N. N. Kuzmin, and S. K. Sidorov, *J. Magn. Magn. Mater.* **1**, 91 (1975).
- ¹⁷T. H. Kim, M. C. Cadeville, A. Dinia, V. Pierron-Bohnes, and H. Rakoto, *Phys. Rev. B* **54**, 3408 (1996).
- ¹⁸Ch. Böttger, R. Stasch, A. Wulfes, and J. Hesse, *J. Magn. Magn. Mater.* **99**, 280 (1991).
- ¹⁹A. Z. Menshikov, G. A. Takzei, Y. A. Dorofeev, V. A. Kazantsev, A. K. Kostyshin, and I. I. Sych, *Sov. Phys. JETP* **62**, 734 (1985); K. Ishida and T. Nishizawa, *Bull. Alloy Phase Diagrams* **11**, 125 (1990).
- ²⁰D. J. Rogers, Y. Maeda, and K. Takei, *J. Appl. Phys.* **78**, 5482 (1995).
- ²¹K. Uchiyama, I. Ishida, E. Hirota, K. Hamada, and A. Okada, *Jpn. J. Appl. Phys.* **36**, 114 (1997).
- ²²J. S. Moodera and J. Mathon, *Annu. Rev. Mater. Sci.* **29**, 381 (1999); P. LeClair, J. T. Kohlepp, H. J. M. Swagten, and W. J. M. de Jonge, *Phys. Rev. Lett.* **86**, 1066 (2001).
- ²³T. Jo and K. Hirai, *J. Phys. Soc. Jpn.* **55**, 2017 (1986).
- ²⁴The diffraction pattern showed good fcc structure for Co ($a = 3.665 \text{ \AA}$), whereas Co-Mn alloys (assuming distorted fcc) showed a change in the a parameter as Mn content increased from 10% to 50%: calculating using the (111) spot gave an a value (3.741–3.766 \AA) slightly smaller than the one obtained using the (200) spot (4.348–3.991 \AA) when Mn percentage increased [if we assume, however, that it is fct structure we get $a = 4.348 \text{ \AA}$ and $c = 2.566 \text{ \AA}$ for $\text{Co}_{0.9}\text{Mn}_{0.1}$ as an example].
- ²⁵Y. Nakai, K. Hozaki, and N. Kunitomi, *J. Phys. Soc. Jpn.* **45**, 73 (1978).
- ²⁶J. W. Cable and Y. Tsunoda, *Phys. Rev. B* **50**, 9200 (1994).
- ²⁷S. Banerjee, W. L. O'Brien, and B. P. Toner, *J. Magn. Magn. Mater.* **198–199**, 267 (1999).
- ²⁸D. A. Arena (private communication).
- ²⁹R. W. G. Wyckoff, *Crystal Structures* (Wiley, New York, 1963), pp. 50–52.
- ³⁰M. B. Stearns, *Phys. Today* **31** (4), 34 (1978).
- ³¹T. Jo and H. Miwa, *J. Phys. Soc. Jpn.* **40**, 706 (1976).